Biomaterials 29 (2008) 4187–4194

Contents lists available at ScienceDirect

Biomaterials

journal homepage: www.elsevier.com/locate/biomaterials

The expression of cross-linked elastin by rabbit blood vessel smooth muscle cells cultured in polyhydroxyalkanoate scaffolds

Shao-Ting Cheng [a], Zhi-Fei Chen [a], Guo-Qiang Chen [a,b,*]

[a] Multidisciplinary Research Center, Shantou University, Shantou 515063, Guangdong, China
[b] Department of Biological Science and Biotechnology, Tsinghua University, Beijing 100084, China

ARTICLE INFO

Article history:
Received 1 July 2008
Accepted 15 July 2008
Available online 6 August 2008

Keywords:
PHB
P3HB4HB
Scaffold
Blood vessel
Elastin
RaSMCs

ABSTRACT

In order to evaluate the possibility for making artificial blood vessels, a series of microbial copolyesters poly(3-hydroxybutyrate-*co*-4-hydroxybutyrate)s (P3HB4HB)s containing 0–40 mol% 4-hydroxybutyrate (4HB) were studied for growth and formation of elastin of rabbit blood vessel smooth muscle cells (RaSMCs) incubated on the solvent-casting polyester films. Porous scaffolds of all P3HB4HBs except P(HB-40 mol% 4HB) were used to compare their potentials as materials for tissue engineering blood vessel (TEBV). The polyesters were studied using static contact angles, differential scanning calorimetry (DSC), cell count kit-8 (CCK-8) and Fastin elastin assays. Simultaneously, SEM, H&E and DAPI staining were employed to study cell morphology and cell growth in the polyester scaffolds. Viability of rabbit blood vessel smooth muscle cells (RaSMCs) grown on P(HB-7 mol% 4HB) films was the strongest among all other tested polyester films during the whole growth process. H&E and DAPI staining clearly suggested good cells' growth and even confluent growth in the P3HB4HB scaffolds. Fastin elastin assay demonstrated that 4HB component in the P3HB4HB copolymer benefited the elastin formation and accumulation. P(HB-20 mol% 4HB) showed a 160% more elastin production compared with that on the well-studied poly(3-hydroxybutyrate-*co*-12 mol% 3-hydroxyhexanoate) (PHBHHx) incubated under the same conditions. Since the P3HB4HB has adjustable elasticity and strength, combined with its ability to induce elastin formation, it can be regarded as a useful material for developing into a material for artificial blood vessels.

1. Introduction

Blood vessel diseases have resulted in increasing mortality worldwide [1–3]. Among all the treatments for blood vessel diseases, tissue engineering (TE) is a promising method [4]. Functional TE blood vessels (TEBVs) combining viable cells and polymer scaffolds as substitutes for the pathological blood vessels would be an efficient approach for clinical applications [5]. Chemically synthesized polymers like polyglycolic acid (PGA), poly(L-lactic acid) (PLLA) and poly(L-lactide-*co*-glycolide) (PLGA), together with the natural macromolecules like polysaccharides, collagen, gelatin and polyhydroxyalkanoates (PHAs) have been widely studied as scaffolds for TE applications [6–9].

A desirable blood vessel scaffold should satisfy the following criteria: (1) good mechanical properties initially and biodegradability after full growth of the blood vessel constituting cells; (2) ability to support cell growth and remodeling; (3) no promotion of stenosis, thrombosis, calcification and infection [10–12].

Polyhydroxyalkanoates (PHAs) are a family of biopolyesters synthesized by many bacteria. PHA has been studied as tissue engineering materials for many applications [8,9]. Similar to two PHAs produced in large scale, namely, poly(3-hydroxybutyrate-*co*-3-hydroxyvalerate) (PHBV) [13] and poly(3-hydroxybutyrate-*co*-3-hydroxyhexanoate) (PHBHHx) [14], P3HB4HB copolyesters consisting of 3-hydroxybutyrate (3HB) and 4-hydroxybutyrate have flexible mechanical properties compared with homopolymer poly-3-hydroxybutyrate (PHB); P3HB4HB is now available in sufficient quantity due to the recent Tianjin Green Bioscience and DSM joint venture (DSM News Release). When P3HB4HB contains 3–8 mol% 4-hydroxybutyrate, it has an extension to break of 45% to over 100%, which are similar to cardiovascular tissues including blood vessels and heart valves [15]. Some studies were conducted for application of P3HB4HB in tissue engineering of heart valves [16], aortic tissue [17] and pulmonary artery [18].

Rabbit blood vessel smooth muscle cells or RaSMCs were the other indispensable part of the artificial blood vessels responsible for contractility, mechanical stability and formation of extracellular matrix (ECM) [19]. Consequently, a suitable substitute to support

* Corresponding author. Multidisciplinary Research Center, Shantou University, Shantou 515063, Guangdong, China. Tel.: +86 754 82903696; fax: +86 754 2901175.
E-mail address: chengq@stu.edu.cn (G.-Q. Chen).

0142-9612/$ – see front matter © 2008 Published by Elsevier Ltd.
doi:10.1016/j.biomaterials.2008.07.022

RaSMCs' proliferation and to form the stretchy ECM rich with elastin similar to a native blood vessel is important for the TEBV elasticity and functionality. Tropoelastin, a soluble protein secreted by RaSMCs in native artery, could become cross-linked to form mature elastin after posttranslational modifications in the ECM [20]. Besides collagen, elastin is a dominant ECM protein deposited in the arterial walls [21]. Elastin is assembled as elastic fibers, conferring elasticity to the connecting tissues, including arterial walls, lungs, ligaments and skins [21–24]. It had been reported that TEBV dilated after the *in vivo* scaffold biodegradation without formation of sufficient elastic fibers [17]. TEBV dilatation could result in thrombosis and other syndromes [25]. Cells lacking elastin could proliferate faster than normal RaSMCs; they could fail to change from a synthetic phenotype to a mature contractile phenotype [21,26]. Therefore, it has been a great challenge to promote elastin synthesis in the TEBV.

In this paper, for the first time, we compared the expression of cross-linked elastin of RaSMCs cultured on the various biopolyester films with a focus on P3HB4HB containing different 4HB contents. In addition, the biopolyesters were fabricated into scaffolds with uniform tubes to support RaSMCs' growth and form tunica media of artificial blood vessels, which extended their potential application as TEBV.

2. Materials and methods

2.1. PHA films' preparation

PLA was obtained from Naturework, US (M_w: 120,000 ± 10%), PHB (M_w: 330,000 ± 10%) and P(3HB-12% HHx) (M_w: 440,000 ± 10%; 12% HHx) from Shangdong Lukang, China, and P(3HB-7% 4HB) (M_w: 530,000 ± 10%), P(3HB-12% 4HB) (M_w: 590,000 ± 10%), P(3HB-20% 4HB) (M_w: 810,000 ± 10%) and P(3HB-40% 4HB) (M_w: 440,000 ± 10%) were supplied by Tianjin Green Bioscience, China. All polyester films were prepared by solvent-casting method using 2 wt% of material in chloroform (YongDa Reagent Development Center, Tianjin, China). The polyester solution was placed in a glass dish (18 mm in diameter) to allow solvent evaporation in air at room temperature. The film coated dishes (FCDs) were dried in vacuum at low temperature for 48 h to totally evaporate the solvent. FCDs then were placed in 12-well plates, then sterilized in 75% ethanol for 4 h, and balanced with culture medium overnight before use.

2.2. Contact angle and surface free energy determination

The static contact angles (θ) were measured using the contact angle analyzer (SL600, Solon Information Technology Co., Ltd, Shanghai, China). In detail, 5 μl standard liquid, distilled water or diiodomethane (CH_2I_2; Sigma, USA) were dropped on the film surface and were measured in 10 s. The surface free energy of test films γ_S consisted of separate dispersion γ_S^d and non-dispersion γ_S^{nd}; it could be calculated by the contact angles of two different liquids through harmonic mean equation as given below:

$$\gamma_L(\cos\theta + 1) = 2\left(\gamma_L^d\gamma_S^d\right)^{1/2} + 2\left(\gamma_L^{nd}\gamma_S^{nd}\right)^{1/2}$$

The "γ"s represent surface tension components of standard liquids, where γ_L, γ_L^d, and γ_L^{nd} represent the surface tension, dispersion and non-dispersion component of standard liquids, respectively (Table 1) [27–29].

2.3. Differential scanning calorimetry of polymer films

Differential scanning calorimetry (TA-Q100 DSC, TA, US) was used to study the crystallization behavior of PLA and PHA. Sample weighted 2 mg each was first equilibrated to −60 °C and then heated to 200 °C at a heating rate of 10 °C/min (Run 1). The samples were maintained at 200 °C for 1 min, and were rapidly cooled to −60 °C to obtain low crystallinity specimens. They were again heated at a rate of 10 °C/min to 200 °C (Run 2). The apparent melting temperature (T_m) and the glass transition temperature (T_g) were obtained from the first heating run of DSC thermograms.

Table 1
Surface tension components of H_2O and CH_2I_2

Standard liquids	Surface tension components (mN/m)		
	γ_L	γ_L^d	γ_L^{nd}
H_2O	72.8	22.1	50.7
CH_2I_2	50.8	44.1	6.7

2.4. Cell culture on film coated dishes (FCDs)

The cell line RaSMCs used in the experiments were kindly provided by Microorganism Lab of Tsinghua University (Beijing, China). Cells were cultured in DMEM medium (Gibco, US) supplemented with 10% FBS (Min Hai Bio-engineering, China), 100 U/ml penicillin (Sigma, US) and 100 U/ml streptomycin (Sigma, US) in a CO_2 incubator (Forma 3111, US) supplied with 5% CO_2 at 37 °C. Confluent cells were digested using 0.25% trypsin–0.02% EDTA, followed by centrifugation (1000*g* for 3 min) to harvest the cells. Subsequently, the single cell suspension was used for cell number calculation using haemacytometer 1.0×10^4 cells were added to each FCD, cultivation was conducted for 24, 48, 72 and 96 h. Then, CCK-8 assay was used for cell viability study while SEM for the morphology of cells grown on the resulting films.

2.5. Scanning electron microscopy

Cell-seeded films were washed three times using phosphate buffered saline (PBS; Shanhai Sangon Biological Engineering Technology & Services Co., Ltd, China), then immersed in PBS with 2.5% glutaraldehyde (Alfa Aesar, USA) overnight at 4 °C, followed by dehydration in ethanol gradient (from 30, 50, 70, 90, 95 to 100%) for 15 min each. The dehydrated cell-seeded films were dried via lyophilization. Then samples of cell-seeded films with these pre-treatments were mounted on aluminum stumps, coated with gold in an auto fine coater (JFC-1600, Japan) for 10 min and examined under a scanning electron microscope (JSM-6360LA, Nikon, Japan). No cell-seeded film without the above treatments was used as control.

2.6. Cell viability

A cell count kit-8 (CCK-8 Beyotime, China) was employed in this experiment to quantitatively evaluate the cell viability. After RaSMCs were inoculated on the FCD for 24, 48, 72 and 96 h, the original medium was replaced by 500 μl 10% FBS DMEM medium contain 50 μl CCK-8. It was incubated at 37 °C for 2 h to form water dissoluble formazan. Then 100 μl of the above formazan solution were taken from each sample and added to one well of a 96-well plate, six parallel replicates were prepared. The absorbances at 450 and 630 nm (calibrated wave) were determined using a microplate reader (Multiskan MK33, Thermo electron corporation, China). DMEM containing 10% CCK-8 was used as a control.

2.7. Fabrication of PHA scaffolds

PHA scaffolds were fabricated using solid–liquid phase separation as described by Ma et al. [6,30]. Briefly, each 0.8 g of various PHA materials was dissolved in 20 ml 1,4-dioxane and refluxed to form a homogeneous solution. The solution was poured into a glass mold surrounded with adiabatic foam. The mold was placed in liquid nitrogen for 30 min and vacuum lyophilized for 5 days to form the resulting scaffold. SEM was used to study the internal morphology of the PHA scaffolds.

2.8. Cell growth in scaffolds

The scaffolds were sterilized and balanced as described above. They were then placed in the 24-well culture plates before cell inoculation. Subsequently, 1.0×10^6 cells were added to each sterilized scaffold to allow their full attachment to the scaffolds. Culture medium was changed every 3 days. Cultivation was conducted for 3 and 7 days. Cell morphology and growth in the scaffolds were studied using SEM.

2.9. Cell-scaffold staining

After the cultivation process lasting 7 days, cell-scaffolds were frozen in liquid nitrogen for 30 min. Subsequently, cell-scaffolds were embedded in gel and 20 μm thick sections were prepared. Harris & Eosin (H&E) was used to stain the cells for studying the cell distribution in the scaffolds.

Scaffold sections were placed in a moist chamber and DAPI was applied to stain the karyons. After incubation at 37 °C for 30 min, slides (scaffold sections) were washed with PBS, and then embedded using the mounting medium containing 30% glycerol and 12% polyvinyl alcohol. The DAPI stained cells were observed using a fluorescence microscope (ECLIPSE TE2000-U, Nikon, Japan).

2.10. Quantitative analysis of insoluble cross-linked elastin (IE) and soluble elastin (SE)

High-performance liquid chromatography (HPLC) is a conventional method used to detect the amount of pentapeptide valyl-glycyl-valyl-prolyl-glycine (VGVPG), or desmosine and isodesmosine derived from elastin [24,31–34]. In this study, a commercially available assay kit (Fastin elastin assay kit, Biocolor, USA) was used to quantitatively assay the amount of cross-linked elastin from the cell layers every 4 days. Total analysis period was 16 days.

Table 2
Contact angles on the tested biopolyester films

Tested films	Contact angles (°)	
	H_2O	CH_2I_2
PLA	76.8 ± 0.4	36.5 ± 1.7
PHB	85.6 ± 0.2	40.3 ± 0.1
P(HB-12% HHx)	88.0 ± 0.5	33.4 ± 0.4
P(HB-7% 4HB)	78.2 ± 1.0	38.4 ± 0.4
P(HB-12% 4HB)	77.5 ± 0.5	30.5 ± 0.6
P(HB-20% 4HB)	72.0 ± 0.3	31.5 ± 0.3
P(HB-40% 4HB)	59.0 ± 0.2	32.5 ± 0.3

Mature cross-linked elastin which is insoluble (IE) and immature cross-linked elastin which is soluble (SE) were prepared as described by Ramamurthi and Vesely [4]. 5–500 μl of culture samples were centrifuged at 12,000*g* for 10 min and precipitated pellets were collected. One milliliter of dye reagent (TPPS-5,10,15,20-tetraphenyl-21,23-porphine sulphonate) was added to each pellet sample collected. They were mixed for 90 min. The dye-bound elastin was collected via centrifugation at 12,000*g* for 10 min. Subsequently, they were destained with a dye dissociation reagent. The absorbance of recovered dye from each sample/standard at 513 nm was assayed using a nucleic acid/protein analyzer (Bckman coulter DU800, German).

2.11. Statistical analysis

All quantitative results were obtained from triplicate samples or more. Data were expressed as the mean ± SD. Statistical analysis was carried out using the unpaired Student's *t* test (Excel, Microsoft, US). A value of $p < 0.05$ was considered to be statistically significant.

3. Results

3.1. Surface property study via contact angle and surface free energy (SFE) measurements

Surface properties strongly affect biocompatibility of a polymer. By using water and CH_2I_2, hydrophilic properties of the biopolyester films can be studied. The most hydrophobic film was found with P(HB-12 mol% HHx), shortly as P(HB-12% HHx), which showed its largest water contact angle among all polyester films studied (Table 2), while P(HB-40% 4HB) showed the strongest hydrophilicity with the smallest water contact angle of 59°. It can be clearly found that P3HB4HB becomes more hydrophilic with increasing 4HB contents (Table 2).

Among all PHA biopolyesters studied, PHB showed the lowest surface free energy (SFE) and P(3HB-40% 4HB) the highest (Fig. 1). SFE increased with increasing 4HB content from 0 to 40%. The non-dispersion component contributed the most to the total surface free energy with the polarity the least. The SFE of the biopolyester films can be found to be in the order of: PHB < P(HB-12% HHx) < PLA < P(3HB-7% 4HB) < P(3HB-12% 4HB) < P(3HB-20% 4HB) < P(3HB-40% 4HB), it showed an opposite trend to the polarity (Fig. 1).

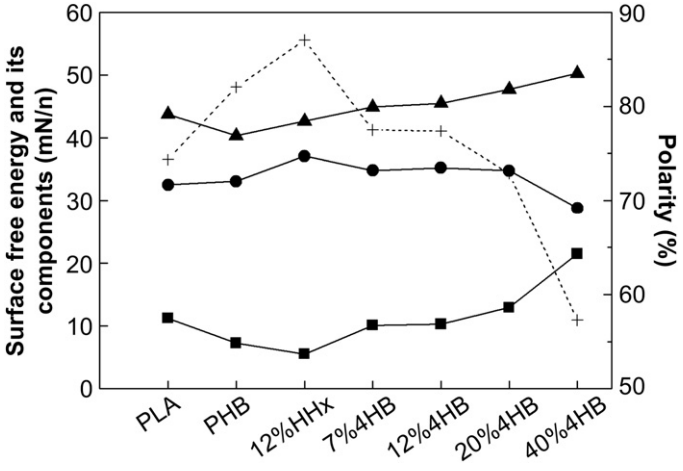

Fig. 1. Surface free energy (SFE) (▲), dispersion component (■), non-dispersion component (●) and the polarity (+) on test films. SFE was the sum of non-dispersion component and dispersion component, and the polarity was the ratio of non-dispersion component to total surface free energy.

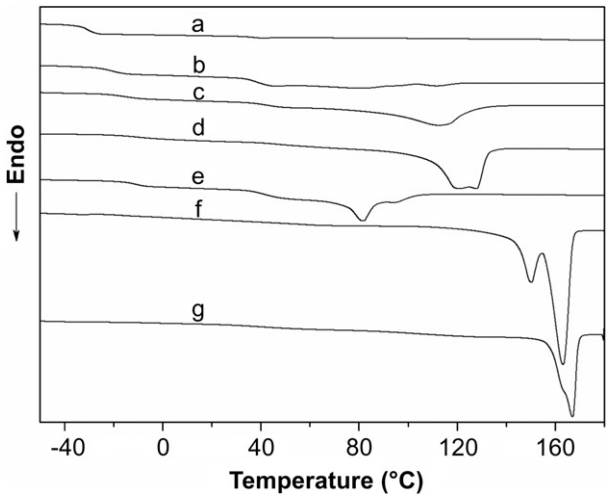

Fig. 2. Differential scanning calorimeter (DSC) analysis of P3HB4HB with (a) 40% 4HB, (b) 20% 4HB, (c) 12% 4HB, (d) 7% 4HB, (e) P(HB-12% HHx), (f) PHB and (g) PLA.

3.2. DSC studies of PLA and PHA films

P3HB4HB containing 12 mol% 4HB (shortly as 12% 4HB) and over demonstrated a completely amorphous state without a clear melting temperature T_m after the melt-quenched process (Fig. 2). The first heating run in the DSC thermograms was used to determine the glass temperature T_g, T_m and melting enthalpy ΔH_m of all tested biopolyester films. The maximum melting temperature was revealed as T_m due to multiple-meting points of some PHA (Fig. 2). With the 4HB content increased from 7 to 40%, T_g of P3HB4HB was found to decrease from 1.0 to −20.8 °C and the T_m from 138.0 to 50.6 °C (Table 3), accompanied by a decreasing crystallinity (X_c%) from 45.2 to 0.5%. Obviously increasing 4HB content destroyed the crystallinity of the perfect PHB crystals [35]. Such a change in crystallinity can also affect surface free energy of a polymer, leading to a changing biocompatibility [29].

3.3. Viability of RaSMCs

No significant growth difference was observed after 24 h of incubation. Growth began to show remarkable differences for the

Table 3
DSC study on thermal properties of PLA and PHA films

PLA or PHA	T_g (°C) [a]	T_m (°C) [a]	ΔH_m (J/g) [a]	X_c% [b]
PLA	47.0	165.5	40.8	43.6
PHB	−6.3	173.0	87.0	59.3
P(HB-12% HHx)	−0.7	104.9	42.5	29.0
P(HB-7% 4HB)	1.0	138.0	66.2	45.2
P(HB-12% 4HB)	−5.1	122.5	52.1	35.5
P(HB-20% 4HB)	−11.0	122.0	31.3	21.4
P(HB-40% 4HB)	−20.8	50.6	0.7	0.5

[a] Glass transition temperature (T_g), melting temperature (T_m) and melting enthalpy (ΔH_m) were studied using DSC from first heating run. The maximum melting temperature was revealed as T_m corresponding to the multiple-melting of PHA films. ΔH_m was obtained from intensities of the endothermal peaks in the DSC first heating run.

[b] Crystallinity was calculated from the melting enthalpy in DSC thermogram. Reference value of completely crystallized PHB [28] was 146.6 J/g (ΔH_m^{θ},PHB), 100% crystallinity of PLA [36] was 93.6 J/g (ΔH_m^{θ},PLA). $X_c\% = 100 \times \Delta H_m/\Delta H_m^{\theta}$.

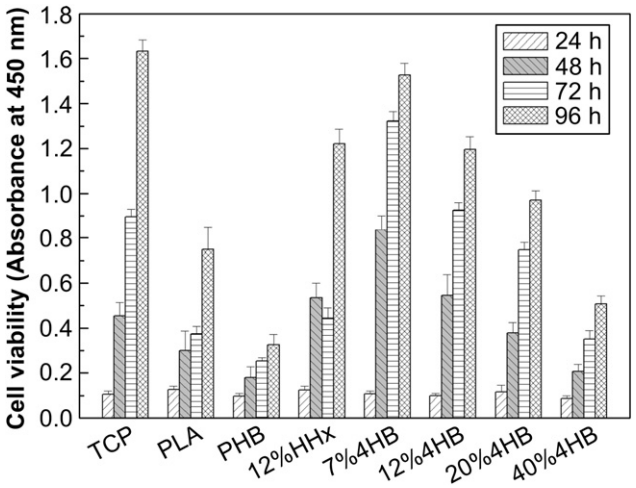

Fig. 3. CCK-8 assays of RaSMCs' proliferation on tested films after 24, 48, 72 and 96 h of incubation.

RaSMCs incubated on different polyester films for 48, 72 and 96 h based on the CCK-8 assay (Fig. 3). PHB showed the poorest cell viability among all tested materials; P(3HB-40% 4HB) did not have a significant growth improvement either. Cells grew the strongest on P(3HB-7% 4HB) in all time period except 24 h, they lost a little viability to become second only to the tissue culture plate (TCP) after 96 h, possibly due to the aging of the cells after a fast growth period. Interesting, cell viability was observed to decrease with increasing 4HB content in the copolymer P3HB4HB from 48 to 96 h. P(HB-12% HHx), as expected, demonstrated a better ability to maintain cell viability than that of PLA and PHB [27]. After 96 h, cell growth on P(HB-12% HHx) was similar to P(3HB-12% 4HB), better than on PLA, PHB, P(3HB-20% 4HB) and P(3HB-40% 4HB).

Some studies showed that RaSMCs cultured on PHA films expressed their cell specific antigens, indicating that the cells grown on PHA did not differentiate [36], although the cell morphology changed obviously from a non-contractile phenotype to a quiescent contractile phenotype during the cultivation process, suggesting a conversion of the cells grown on the films from pathological to physiological states (pictures not shown) [37,38].

3.4. Growth of RaSMCs in PHA scaffolds

Regular tubing structures were clearly observed in PHA scaffolds (Fig. 4). All scaffold tubes point to the same direction, they also appeared with homogeneous diameters ranging from 60 to 100 μm. PHB scaffold was found to be brittle and not suitable for further development, therefore, the well-studied P(HB-12% HHx) was used as a control for this research although their tubes had a little smaller diameters compared with that of P3HB4HB [30]. Cell growth was observed inside all tested PHA scaffolds. After 7 days of incubation, the cell density was found higher enough to form confluence inside all the PHA scaffolds, while only individual cells were observed for a 3-day growth period inside all scaffolds (Fig. 5). DAPI and H&E staining seemed to reveal a higher cell density cells in the P3HB4HB scaffolds compared with that in the PHBHHx ones (Fig. 6). The larger P3HB4HB diameters may be one of the reasons for the favorable cell growth compared with the smaller diameters in the PHBHHx scaffold tubes.

3.5. Fastin elastin assay

After the growth of RaSMCs on the biopolyester films for 4–16 days, IE and SE produced by the cells grown on different materials were quantitatively studied using Fastin assay (Fig. 7 and Table 4). IE formation was observed to be the strongest on P(3HB-12% 4HB) for the first 4 days, with the weakest on P(3HB-40% 4HB). After 12 days, IE reached its maximum in quantity on P(3HB-20% 4HB) among all tested films. In all cases, a reduction on IE formation was observed after 16 days. Surprisingly, the well-studied and characterized PHBHHx was the least favor material for IE formation. On day 4, the highest IE amount was found on the P(3HB-12% 4HB). Otherwise, IE had the weakest formation on P(3HB-40% 4HB) on

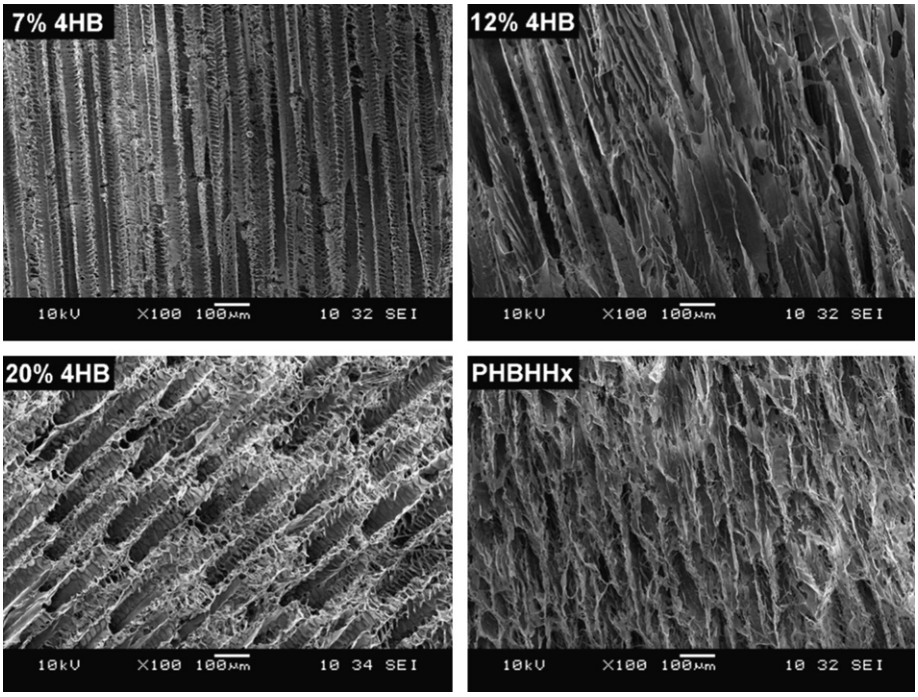

Fig. 4. Morphology of the sections of PHA scaffolds. The scale bar is 100 μm.

day 4. It appeared that increasing 4HB content had a tendency to promote IE formation, although over production of IE led to a reduction in late period of time. Apparently this was related to cell aging that also resulted in reduction of IE formation.

SE, the immature cross-linked elastin, is the transient state between tropoelastin and IE [4]. During the whole incubation process, the contents of SE changed among all samples at each detection time, ranging only from 2 to 8 μg/well, suggesting that the posttranslational modifications of elastin synthesized by RaSMCs on different films were different during the same culture period (Table 4). It was therefore proposed that the total amount of IE was depended on the tropoelastin quantity when the SE was stably synthesized (Table 4). Remarkably, P3HB4HB containing 7 and 12% 4HB produced the most SE after 16 days of incubation.

4. Discussion

PHAs are a diverse biopolyesters with flexible properties depending on their monomer structures and contents [36]. Among many PHAs, P3HB4HB becomes available in sufficient quantity for application research. Although PHAs have been exploited as tissue engineering materials [8], only little study using PHA was conducted for artificial blood vessel application. Therefore, a flexible P3HB4HB is naturally an interesting material for exploitation as a candidate material for making tissue engineering blood vessel (TEBV). P3HB4HBs are typical semicrystallized copolyesters with 4HB as an amorphous component [39]. T_g and T_m of P3HB4HB become wider and more unconspicuous whilst the degree of X_c% diminishes with increasing 4HB content (Table 3 and Fig. 3).

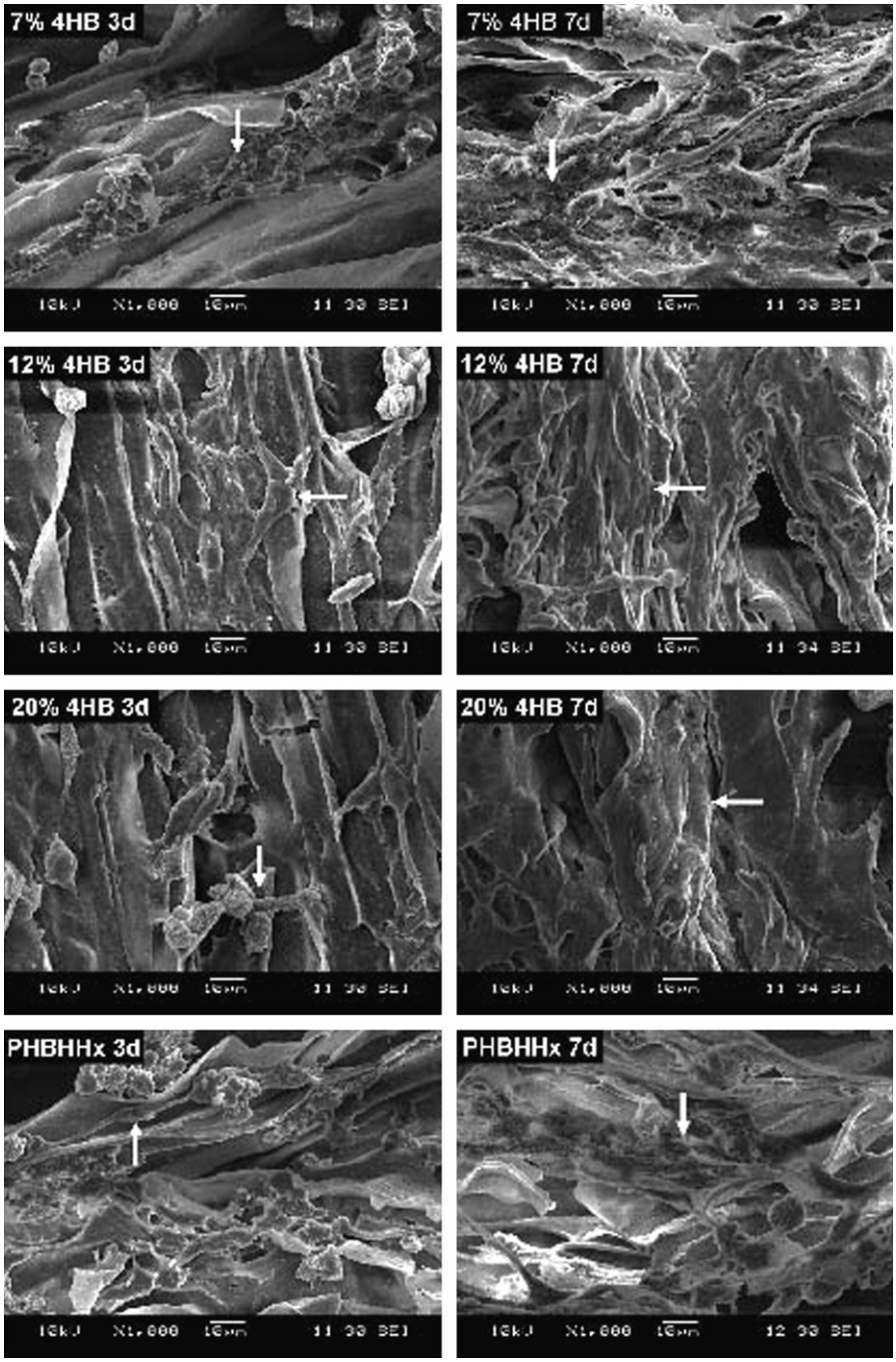

Fig. 5. Morphology of RaSMCs cultured in scaffolds for 3 and 7 days. White arrows point to cells attached on the wall of the scaffold tubes. The scale bar is 10 μm.

Crystallization behaviors of a polymer play an important role in changing its surface physicochemical properties including hydrophilicity, surface free energy, and polarity [29]. In this study, increasing 4HB in the copolymers led to increasing polymer surface free energy and decreasing polarity (Fig. 1 and Table 2), both factors combined to increase the hydrophilicity of the P3HB4HB (Table 2), leading to adjustable biocompatibility.

The interaction between cells and a material surface contributes partially to material biocompatibility [40,41]. Usually, a hydrophilic interface is regarded as beneficial for cell adhesion and proliferation [42]. However, this is not always the case [27], crystallization rate could govern the cellular responses too [29]. For instance, P(HB-12% HHx) is more hydrophobic than PHB yet PHBHHx has a better biocompatibility than PHB does [29,36].

Low crystallization degree and rapid crystallization rate usually generate a smooth surface which improves the attachment and growth of some mammalian cells [43]. For RaSMCs, the crystallization degree (X_c%) at 45% was found to support cell growth the strongest (Fig. 3), this corresponds to a 7% 4HB in P3HB4HB (Table 3). With the X_c% decreased continuously, RaSMCs viability decreased accordingly (Table 3 and Fig. 3). On the other hand, material surface morphology and cell type jointly decide the cell viability and growth behaviors [43,44]. RaSMCs cultured on P(3HB-7% 4HB) films and scaffolds proliferated the best (Figs. 3 and 5), they also grew well in all P3HB4HB scaffolds (Figs. 5 and 6). The hydrophilicity of all P3HB4HB on their films and inside the scaffolds may play a role in promoting the cell growth (Table 2 and Figs. 3, 5 and 6). Beside the surface structures and material inherent

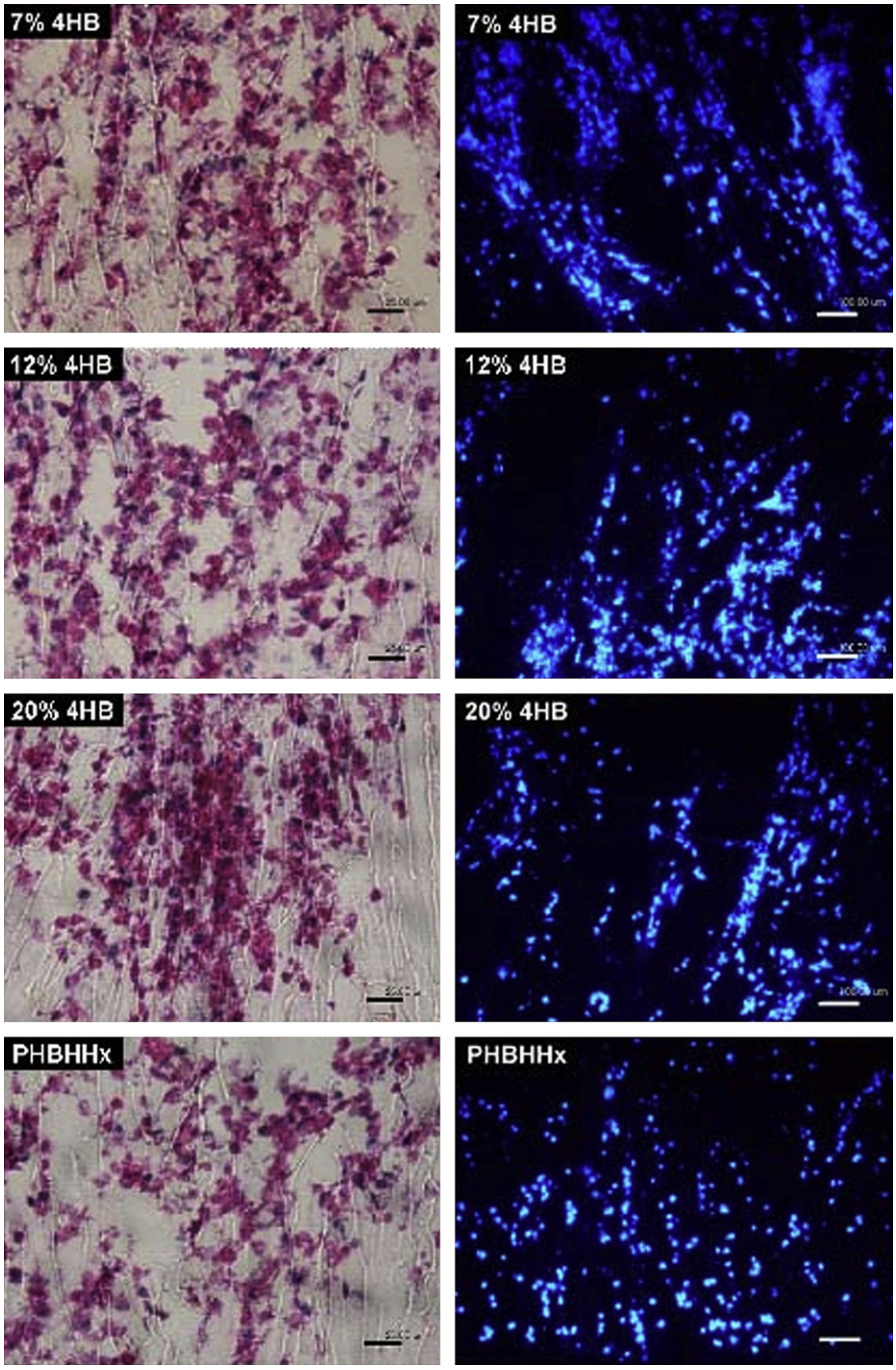

Fig. 6. Distribution of RaSMCs in PHA scaffolds at 7 days. Histological sections of PHA scaffolds were stained using H&E (left, bar = 25 μm) and DAPI (right, bar = 100 μm).

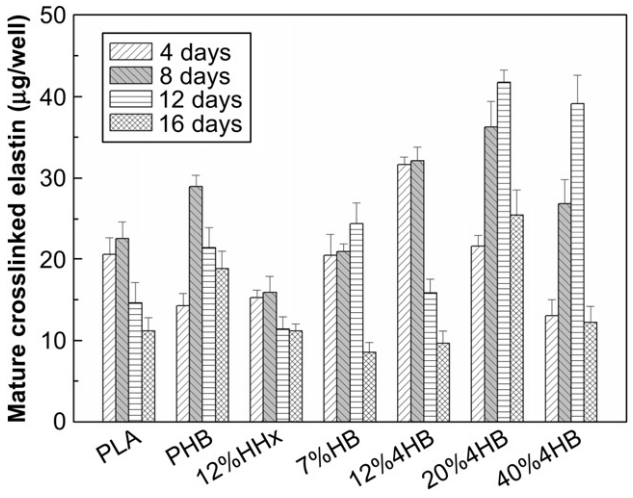

Fig. 7. Synthesis of extracellular matrix mature elastin (IE). Shown are the mean ± SD ($n = 3$) of the amounts of elastin derived from RaSMCs cultured on PLA and PHA films for up to 16 days.

properties, the diameters of the scaffold tubes are another crucial factor affecting the cell growth, a wider aperture may allow easy access for cell ingrowth and help exchange of nutrients and oxygen for the cells residing inside the scaffolds (Figs. 4–6). Moreover, this type of scaffold facilitates RaSMCs to orient relevant tissue, particularly the vessel tunica media with sufficient internal elastic lamina, this could lead to the eventual functionalization of the blood vessel [45,46].

1.0×10 cells/well was inoculated on the test films because high initial cell number would not be helpful for elastin synthesis [22,23]. In addition, different materials and seeding methods could influence the matrix components [4,47]. Elastin formation and degradation are specific states of physiological equilibrium when RaSMCs are in the quiescent contractile phenotype. Elastin can be degraded by elastase secreted during the cell migration [48]. In the 4-day cultures, cells' growth on P(HB-12% HHx) and P(3HB-12% 4HB) scaffolds had similar activity, yet the latter one had better ability to IE synthesis, suggesting that the presence of 4HB was positive for IE formation (Fig. 7). Throughout the 16-day incubation period, Fastin elastin assay showed that cells grown on P3HB4HB were 50 to 160% more in producing IE compared with P(HB-12% HHx), suggesting that 4HB component had an ability to stimulate elastin in RaSMCs steadily. Since the DNA sequence of gene encoding rabbit elastin has still not been known, it is thus not possible to measure the level of tropoelastin mRNA at this stage. However, the above results allow us to conclude that P3HB4HB is a promising tissue engineering material for blood vessel reconstruction due to its good biocompatibility including ability to promote elastin formation, their strong elasticity and biodegradability [49].

Table 4
Synthesis of extracellular matrix immature cross-link elastin (SE) on various films

Film materials	Immature cross-link elastin SE (μg/well)			
	4 days	8 days	12 days	16 days
PLA	2.63 ± 0.26	1.79 ± 0.13	2.05 ± 0.34	2.79 ± 0.38
PHB	2.99 ± 0.46	2.29 ± 0.26	2.77 ± 0.24	3.06 ± 0.41
P(HB-12% HHx)	3.71 ± 0.25	2.69 ± 0.43	2.19 ± 0.29	3.54 ± 0.49
P(HB-7% 4HB)	5.27 ± 0.46	4.65 ± 0.46	4.00 ± 0.16	7.57 ± 0.21
P(HB-12% 4HB)	3.82 ± 0.34	2.82 ± 0.41	4.10 ± 0.42	8.39 ± 0.31
P(HB-20% 4HB)	2.82 ± 0.29	2.10 ± 0.38	3.43 ± 0.31	6.43 ± 0.13
P(HB-40% 4HB)	2.33 ± 0.31	2.22 ± 0.31	2.06 ± 0.21	6.31 ± 0.19

SE was prepared as described by Ramamurthi and Vesely [4]. For more details see Section 2.10.

5. Conclusion

RaSMCs behaved differently on P3HB4HB series copolyesters. Using the well-studied P(HB-12% HHx) as a control, cells grew the best on P(3HB-7% 4HB) films and in all the P3HB4HB scaffolds. The results of Fastin elastin assay for RaSMCs on the biopolyester films demonstrated that 4HB component could stimulate formation of elastin. Furthermore, P3HB4HB films showed 50–160% higher elastin formation, together with a longer elastin production period than P(HB-12% HHx). Consequently, P3HB4HB demonstrated a strong potential to be developed into tissue engineering blood vessels containing high levels of mature elastin.

Acknowledgement

The research was supported by Li Ka Shing Foundation and National High Tech 863 Grant (Project Nos. 2006AA02Z242 and 2006AA020104), as well as the State Basic Science Foundation 973 (2007CB707804). Guangdong Provincial Grant for collaboration among industry, university and research organization awarded to GQC has also contributed to this study.

References

[1] Spiel AO, Gilbert JC, Jilma B. von Willebrand factor in cardiovascular disease: focus on acute coronary syndromes. Circulation 2008;117:1449–59.
[2] Park MH. Advances in diagnosis and treatment in patients with pulmonary arterial hypertension. Catheter Cardiovasc Interv 2008;71:205–13.
[3] Tain YL. Endothelial dysfunction links cardiovascular disease to pediatric chronic kidney disease: the role of nitric oxide deficiency. Acta Paediatr Taiwan 2007;48:246–50.
[4] Ramamurthi A, Vesely I. Evaluation of the matrix-synthesis potential of crosslinked hyaluronan gels for tissue engineering of aortic heart valves. Biomaterials 2005;26:999–1010.
[5] Yang J, Motlagh D, Webb AR, Ameer GA. Novel biphasic elastomeric scaffold for small-diameter blood vessel tissue engineering. Tissue Eng 2005;11:1876–86.
[6] Ma PX. Scaffolds for tissue fabrication. Mater Today 2004;7:30–40.
[7] Mooney DJ, Mazzoni CL. Stabilized polyglycolic acid fibre based tubes for tissue engineering. Biomaterials 1996;17:115–24.
[8] Chen GQ, Wu Q. The application of polyhydroxyalkanoates as tissue engineering materials. Biomaterials 2005;26:6565–78.
[9] Williams SF, Martin DP, Horowitz DM, Peoples OP. PHA applications: addressing the price performance issue I. Tissue engineering. Int J Biol Macromol 1999;25:111–21.
[10] Seifalian AM, Tiwari A, Hamilton G, Salacinski HJ. Improving the clinical patency of prosthetic vascular and coronary bypass grafts: the role of seeding and tissue engineering. Artif Organs 2002;26:307–20.
[11] Rhima C, Niklason LE. Tissue engineered vessels: cells to telomeres. Prog Pediatr Cardiol 2006;21:185–91.
[12] Suma H. Arterial grafts in coronary bypass surgery. Ann Thorac Cardiovasc Surg 1999;5:141–5.
[13] Rivard CH, Chaput C, Rhalmi S, Selmani A. Bioabsorbable synthetic polyesters and tissue regeneration. A study of three-dimensional proliferation of oven chondrocytes and psteoblasts. Ann Chir 1996;50:651–8.
[14] Wang YW, Wu Q, Chen GQ. Attachment, proliferation and differentiation of osteoblasts on random biopolyester poly(3-hydroxybutyrate-*co*-3-hydroxyhexanoate) scaffolds. Biomaterials 2004;25:669–75.
[15] Williams SF, Sherborn MA. Bioabsorbable, biocompatible polymers for tissue engineering. US Patent no. 6514515; 2003.
[16] Sodian R, Hoerstrup SP, Sperling JS, Daebritz SH, Martin DP, Schoen FJ, et al. Tissue engineering of heart valves: in vitro experiences. Ann Thorac Surg 2000;70:140–4.
[17] Opitz F, Schenke-Layland K, Cohnert TU, Starcher B, Halbhuber KJ, Martin DP, et al. Tissue engineering of aortic tissue: dire consequence of suboptimal elastic fiber synthesis *in vivo*. Cardiovasc Res 2004;63:719–30.
[18] Stock UA, Sakamoto T, Hatsuoka S, Martin DP, Nagashima M, Moran AM, et al. Patch augmentation of the pulmonary artery with bioabsorbable polymers and autologous cell seeding. J Thorac Cardiovasc Surg 2000;120:1158–67.
[19] Opitz F, Schenke-Layland K, Richter W, Martin DP, Degenkolbe I, Wahlers T, et al. Tissue engineering of ovine aortic blood vessel substitutes using applied shear stress and enzymatically derived vascular smooth muscle cells. Ann Biomed Eng 2004;32:212–22.
[20] Bochicchio B, Floquet N, Pepe A, Alix AJP, Tamburro AM. Dissection of human tropoelastin: solution structure, dynamics and self-assembly of the exon 5 peptide. Chem Eur J 2004;10:3166–76.
[21] Patel A, Fine B, Sandig M, Mequanint K. Elastin biosynthesis: the missing link in tissue-engineered blood vessels. Cardiovasc Res 2006;71:40–9.
[22] Long JL, Tranquillo RT. Elastic fiber production in cardiovascular tissue-equivalents. Matrix Biol 2003;22:339–50.

[23] Mecham RP, Madaras JG, Senior RM. Extracellular matrix-specific induction of elastogenic differentiation and maintenance of phenotypic stability in bovine ligament fibroblasts. J Cell Biol 1984;98:1804–12.
[24] Yanmaguchi Y, Haginaka J, Kunitomo M, Yasuda H, Bando Y. High-performance liquid chromatographic determination of desmosine and isodesmosine in tissues and its application to studies of alteration of elastin induced by atherosclerosis. J Chromatogr 1987;422:53–9.
[25] Waugh JM, Li-Hawkins J, Yuksel E, Kuo MD, Cifra PN, Hilfiker PR, et al. Thrombomodulin overexpression to limit neointima formation. Circulation 2000;102:332–7.
[26] Seyama Y, Wachi H. Atherosclerosis and matrix dystrophy. J Atheroscler Thromb 2004;11:236–45.
[27] Qu XH, Wu Q, Liang J, Qu X, Wang SG, Chen GQ. Enhanced vascular-related cellular affinity on surface modified copolyesters of 3-hydroxybutyrate and 3-hydroxyhexanoate (PHBHHx). Biomaterials 2005;26:6991–7001.
[28] Yang J, Bei JZ, Wang SG. Enhanced cell affinity of poly (D,L-lactide) by combining plasma treatment with collagen anchorage. Biomaterials 2002; 23:2607–14.
[29] Zheng Z, Bei FF, Tian HL, Chen GQ. Effects of crystallization of polyhydroxyalkanoate blend on surface physicochemical properties and interactions with rabbit articular cartilage chondrocytes. Biomaterials 2005;26: 3537–48.
[30] Ma PX, Zhang RY. Microtubular architecture of biodegradable polymer scaffolds. J Biomed Mater Res 2001;56:469–77.
[31] Martorana PA, Beume R, Lucattelli M, Wollin L, Lungarella G. Roflumilast fully prevents emphysema in mice chronically exposed to cigarette smoke. Am J Respir Crit Care Med 2005;172:848–53.
[32] Soskel NT. High-performance liquid chromatographic quantitation of desmosine plus isodesmosine in elastin and whole tissue hydrolysates. Anal Biochem 1987;160:98–104.
[33] Sandberg LB, Wolt TB, Leslie JG. Quantitation of elastin through measurement of its pentapeptide content. Biochem Biophys Res Commun 1986;136: 672–8.
[34] Ma S, Lieberman S, Turino GM, Lin YY. The detection and quantitation of free desmosine and isodesmosine in human urine and their peptide-bound forms in sputum. Proc Natl Acad Sci U S A 2003;100:12941–3.
[35] Felstein MM, Kuptsov SA, Shandryuk GA. Coherence of thermal transitions in poly(*N*-vinyl pyrrolidone)-poly(ethylene glycol) compatible blends 2. The temperature of maximum cold crystallization rate versus glass transition. Polymer 2000;41:5339–48.
[36] Qu XH, Wu Q, Liang J, Zou B, Chen GQ. Effect of 3-hydroxyhexanoate content in poly(3-hydroxybutyrate-*co*-3-hydroxyhexanoate) on in vitro growth and differentiation of smooth muscle cells. Biomaterials 2006;27:2944–50.
[37] Owens GK, Kumar MS, Wamhoff BR. Molecular regulation of vascular smooth muscle cell differentiation in development and disease. Physiol Rev 2004;84:767–801.
[38] Owens GK. Role of mechanical strain in regulation of differentiation of vascular smooth muscle cells. Circ Res 1996;79:1054–5.
[39] Zhu ZY, Dakwa P, Tapadia P, Whitehouse RS, Wang SQ. Rheological characterization of flow and crystallization behavior of microbial synthesized poly(3-hydroxybutyrate-*co*-4-hydroxybuterate). Macromolecules 2003;36:4891–7.
[40] Yoshinari M, Klinge B, Dérand T. The biocompatibility (cell culture and histologic study) of hydroxyapatite-coated implants created by ion beam dynamic mixing. Clin Oral Implants Res 1996;7:96–100.
[41] Wiese KG, Heinemann DEH, Ostermeier D, Peters JH. Biomaterial properties and biocompatibility in cell culture of a novel self-inflating hydrogel tissue expander. J Biomed Mater Res 2001;54:179–88.
[42] García AJ, Boettiger D. Integrin–fibronectin interactions at the cell–material interface: initial integrin binding and signaling. Biomaterials 1999;20:2427–33.
[43] Zhao K, Deng Y, Chen GQ. Effects of surface morphology on the biocompatibility of polyhydroxyalkanoates. Biochem Eng J 2003;16:115–23.
[44] Yang XS, Zhao K, Chen GQ. Effect of surface treatment on the biocompatibility of microbial polyhydroxyalkanoates. Biomaterials 2002;23:1391–7.
[45] Hoerstrupa SP, Zünd G, Sodianb R, Schnellc AM, Grünenfelder J, Turina MI. Tissue engineering of small caliber vascular graft. Eur J Cardiothorac Surg 2001;20:164–9.
[46] Ma PX, Zhang RY, Xiao GZ. Franceschi. Engineering new bone tissue in vitro on highly porous poly(α-hydroxyl acids)/hydroxyapatite composite scaffolds. J Biomed Mater Res 2001;54:284–93.
[47] Kim BS, Putnam AJ, Kulik TJ, Mooney DJ. Optimizing seeding and culture methods to engineer smooth muscle tissue on biodegradable polymer matrices. Biotechnol Bioeng 1998;57:46–54.
[48] Mann BK, Gobin AS, Tsai AT, Schmedlen RH, West JL. Smooth muscle cell growth in photopolymerized hydrogels with cell adhesive and proteolytically degradable domains: synthetic ECM analogs for tissue engineering. Biomaterials 2001;22:3045–51.
[49] Miller ND, Williams DF. On the biodegradation of poly-beta-hydroxybutyrate homopolymer and poly beta-hydroxybutyrate–hydroxyvalerate copolymers. Biomaterials 1987;8:129–37.